ChemPubSoc Europe

DOI: 10.1002/cbic.201700464

CHEMBIOCHEM Full Papers

SPECIAL ISSUE

Cell Factory Design and Optimization for the Stereoselective Synthesis of Polyhydroxylated Compounds

Thomas Wiesinger[+], Thomas Bayer[+], Sofia Milker, Marko D. Mihovilovic, and Florian Rudroff*[a]

A synthetic cascade for the transformation of primary alcohols into polyhydroxylated compounds in *Escherichia coli*, through the in situ preparation of cytotoxic aldehyde intermediates and subsequent aldolase-mediated C–C bond formation, has been investigated. An enzymatic toolbox consisting of alcohol dehydrogenase AlkJ from *Pseudomonas putida* and the dihydroxyacetone-/hydroxyacetone-accepting aldolase variant Fsa1-A129S was applied. Pathway optimization was performed at the genetic and process levels. Three different arrangements of the *alkJ* and *fsa1-A129S* genes in operon, monocistronic, and pseudo-operon configuration were tested. The last of these proved to be most beneficial with regard to bacterial growth and protein expression levels. The optimized whole-cell catalyst, combined with a refined solid-phase extraction downstream purification protocol, provides diastereomerically pure carbohydrate derivatives that can be isolated in up to 91% yield over two reaction steps.

Introduction

Carbohydrates and their derivatives are key players in cellular processes, such as cell signaling, cellular recognition, bacterial and viral infections, cellular dysfunction, and inflammation.[1] Furthermore, glycoconjugates (e.g., proteins, lipids, metabolites)[2] contribute to structural diversity in biological systems. Their ubiquitous presence in nature has led to increasing interest from the scientific community in the development of novel synthetic strategies for the preparation of sugar derivatives to disclose their biological roles and potential medicinal applications.[3]

Most carbohydrate syntheses are based on modifications of chiral compounds and require elaborate and sometimes complex or atom-inefficient protection/deprotection chemistry.[4] The catalytic and asymmetric aldol reaction offers a powerful alternative for the preparation of polyhydroxylated compounds by installing chiral hydroxyl groups through consecutive carboligation reactions of small molecules.[5] Major achievements were published by various groups, who investigated an organo- and metal-catalyzed sequential aldol reaction for the preparation of hexoses.[6] Recently, the group of Clapés published a similar concept based on the assembly of formaldehyde and glycolaldehyde by biocatalytic tandem aldol reactions in vitro.[7]

Aldolases catalyze the stereoselective addition of a donor molecule (carbon nucleophile) to an acceptor carbon electrophile.[8] The former often is a ketone enolate or an enamine intermediate (depending on class I or II aldolase) and the latter an aldehyde. During this carboligation reaction, up to two chiral centers with defined stereochemistry are introduced in a single reaction step. Whereas most aldolases are strictly specific for their donor nucleophile (e.g., dihydroxyacetone phosphate, pyruvate), they usually display a very relaxed substrate scope for the aldehyde acceptor.[9]

Recent studies by the groups of Fessner and Clapés have demonstrated the power of protein engineering by expanding the substrate, more precisely, the donor scope of aldolases. Both groups modified the specificity of D-fructose-6-phosphate aldolase (FSA) to hydroxyacetone (HA) and dihydroxyacetone (DHA),[10] hydroxyethanal,[11] and a wide variety of more sterically demanding nucleophiles.[10,12] In contrast, a vast number of different aldehydes are accepted.[13] Aldehydes are very strong electrophiles, which can undergo different side reactions, such as the irreversible formation of a Schiff base with the free amino group of the lysine in the active site (class I aldolase), overoxidation to the corresponding carboxylic acid in the presence of alcohol dehydrogenases (ADHs), or polymerization.[14] Such obstacles can be overcome by the in situ production of the aldehyde species, which can be converted concomitantly, in the presence of a donor molecule, to the corresponding aldol adduct. Thus, the aldehyde concentration will be low and side reactions can be reduced. The groups of Clapés and Turner successfully demonstrated this approach in a biocatalytic in vitro cascade composed of an alcohol oxidase/chloroper-

[a] DI T. Wiesinger,[+] Dr. T. Bayer,[+] Dr. S. Milker, Prof. M. D. Mihovilovic, Dr. F. Rudroff
Institute of Applied Synthetic Chemistry, OC-163, TU Wien
Getreidemarkt 9, 1060 Vienna (Austria)
E-mail: florian.rudroff@tuwien.ac.at

[+] These authors contributed equally to this work.

Supporting information and the ORCID identification numbers for the authors of this article can be found under https://doi.org/10.1002/cbic.201700464.

This article is part of a Special Issue on Biocatalysis, which commemorates the BioTrans2017 Symposium in Budapest, Hungary.

oxidase or ADH, wild-type FSA, and a cofactor recycling system for the synthesis of a precursor of D-fagomine.[14,15]

In particular, enzyme cascade catalysis for the production of fine chemicals and bioactive compounds has received significant attention in recent years.[16] Cascade reactions combine different biocatalysts in a one-pot process either in vitro[17] or in vivo,[18] mimicking biosynthetic pathways in nature. No isolation of intermediates is required; toxic intermediates are reduced; reaction equilibria can be shifted in favor of product formation; and, therefore, higher yields and the reduction of waste are achieved. The introduction of synthetic cascades into living organisms, such as *Escherichia coli*, lead to so-called designer cells,[19] which offer advantages over in vitro systems. Tedious enzyme preparation, isolation, and purification can be omitted; no additional cofactor recycling system is required; and tools from synthetic biology and metabolic engineering can be used to optimize carbon flux through the cascade.[20]

Herein, we combined the concepts of artificial enzyme cascades in living cells, the in situ aldehyde production for subsequent stereoselective aldol reaction, and a straightforward isolation and purification protocol.[9a] Two non-natively related enzymes, the membrane-associated ADH AlkJ and the DHA/HA-dependent aldolase variant Fsa1-A129S were coexpressed in *E. coli*. AlkJ oxidized a variety of primary alcohols to the corresponding acceptor aldehydes. In the presence of donor molecules, either DHA or HA, the polyhydroxylated aldol adducts were formed. Pathway optimization was performed at the genetic level through the inclusion of different regulatory elements (e.g., promoters, terminators). Through this study, we extended our previous proof-of-concept work on the synthesis of chiral aldol products in vivo[18a] and provided in-depth optimization at genetic and process levels (Figure 1). Finally, we investigated a fast and very efficient solid-phase extraction (SPE) purification protocol for the isolation of all target molecules in good to excellent yields (see Table 3, below; **1**–**4 d**, **e**).

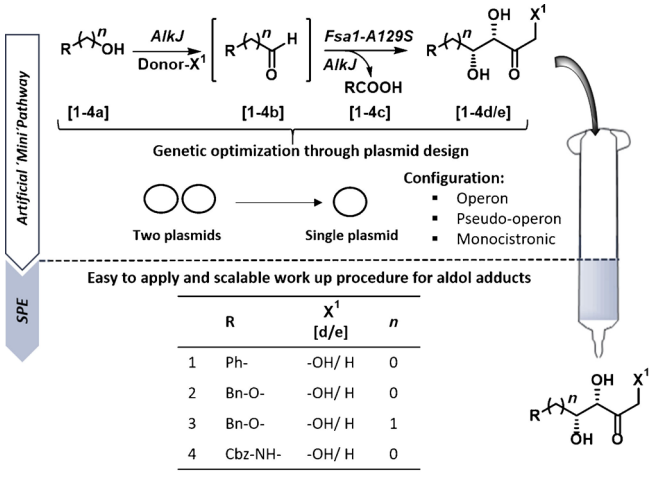

	R	X^1 [d/e]	n
1	Ph-	-OH/ H	0
2	Bn-O-	-OH/ H	0
3	Bn-O-	-OH/ H	1
4	Cbz-NH-	-OH/ H	0

Figure 1. Illustration of the designed process containing an optimized pathway in a whole-cell system and SPE procedure.

Results and Discussion

Identification of suitable enzymes with necessary substrate promiscuity

For a successful cascade setup, catalytic entities with a broad and overlapping substrate profile must be investigated. First, we tested five different ADHs from various species for the oxidation of the primary alcohol target compounds (Table 1).

Table 1. Relative alcohol consumption [%] monitored by GC/flame ionization detection (FID) after 2 h.[a]

Substrate	LK-ADH	RR-ADH	ADH-ht	ADH-a	AlkJ[b]
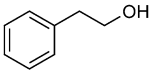	n.c.	n.c.	n.c.	n.c.	>99
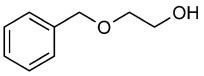	n.c.	n.c.	n.c.	n.c.	>99
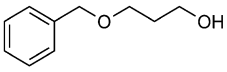	n.c.	n.c.	n.c.	n.c.	>99
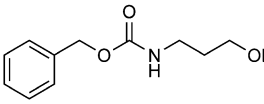	n.c.	n.c.	27	n.c.	>99

[a] n.c.: not converted. [b] 15–20% overoxidation. All reactions were performed in duplicate and the reaction progress was monitored by GC/FID (for reaction conditions, see the Supporting Information).

Analytical-scale whole-cell biotransformations employing LK-ADH from *Lactobacillus kefir*[21] and RR-ADH from *Rhodococcus ruber*[22] did not yield the corresponding aldehydes (Table 1). The thermostable ADH-ht from *Bacillus stearothermophilus*, an ADH with known oxidation activity towards primary alcohols,[23] exclusively accepted the carboxybenzyl (Cbz)-protected amino alcohol (**4 a**) and gave 27% of the desired aldehyde within 2 h reaction time. Furthermore, ADH-a from *R. ruber*, which was predominantly reported for the oxidation of secondary alcohols with few exceptions, such as 2-phenylethanol (**1 a**), showed no activity towards our model substrates.[24] More promising results were obtained by applying AlkJ, an ADH from *Pseudomonas putida*,[25] which was known for the oxidation of aliphatic alcohols. All tested alcohols (**1**–**4 a**) were fully consumed within 2 h reaction time, yielding the corresponding aldehydes. Longer reaction times led to significant overoxidation to the carboxylic acids (up to 80%). Control experiments with *E. coli* BL21(DE3) in the presence of **1 a** showed no endogenous oxidation activity under standard reaction conditions.[18a] Apart from the beneficial substrate uptake velocity of membrane-associated AlkJ, this flavin adenine dinucleotide (FAD)-dependent ADH promotes thermodynamically disfavored alcohol oxidation and takes advantage of irreversible O_2 reduction in the electron transport chain.[20,25,26] With AlkJ, we identified a suitable ADH for the subsequent aldol reaction catalyzed by Fsa1-A129S.

Pathway setup and optimization approaches

Based on the ADH screening, AlkJ turned out to be the most suitable biocatalyst for the oxidation of our aromatic primary alcohols (phenyl- (**1a**), benzyloxy- (**2**–**3a**), Cbz-amino (**4a**) alcohols), which were known aldolase acceptor molecules.[27] To establish the artificial pathway containing AlkJ and engineered Fsa1-A129S, sequence- and ligation-independent cloning (SLIC) methods were applied to assemble the two target genes on a single plasmid for coexpression in the same host. In the following sections, two consecutive optimization strategies were followed. Optimization at the genetic level, with the aim of constructing vectors harboring the *alkJ* and *fsa1-A129S* genes in different genetic configurations (Figure 2), conveniently reduced the plasmid burden from two to a single plasmid. These three configurations differ in the arrangement and number of promotors and terminators. Tuning process parameters followed the detailed characterization of the individual genetic systems to improve the overall performance of the designed pathway (see Figure 4, below).

Vector construction for pathway expression and optimization at the genetic level

Because the expression of heterologous pathways imposes an inherently high metabolic burden on *E. coli* and can impair growth rates, cell viability, and flux through the artificial pathway,[20] the plasmid burden was reduced by the construction of single vectors for the coproduction of AlkJ and Fsa1-A129S. Two methods for vector construction were used: FastCloning (FC)[28] and the application of a seamless and ligation-independent cloning extract (SLiCE).[29] The previously constructed pKA1/*alkJ* plasmid[18a] served as the parent plasmid backbone for the insertion of the *fsa1-A129S* gene in different genetic architectures (Figure 2). In the first round of cloning, the OPE plasmid was constructed by SLiCE to assemble the pKA1/*alkJ* backbone and *fsa1-A129S* fragments in the operon configuration. In our operon, the expression of the two genes is controlled by only one T7 promoter (P_{T7}) in front of the *alkJ* gene and one T7 terminator (T_{T7}) downstream of the aldolase-coding region (Figure 2A). The previously FC-assembled POP plasmid[18a] contains the two genes in pseudo-operon configuration, including an individual P_{T7} in front of the *fsa1-A129S* gene (Figure 2B). Subsequently, a vector with monocistronic arrangement was constructed by molecular cloning (Figure 2C).

Therefore, the unique BamHI restriction site between the coding regions of *alkJ* and *fsa1-A129S* was utilized to insert the unidirectional terminator B0011 (sequence retrieved from http://parts.igem.org/Part:BBa_B0011).

Insertion of the terminator downstream of the *alkJ* stop codon and upstream of the P_{T7} of the aldolase-coding region gave rise to the MON plasmid. Competent *E. coli* BL21(DE3) cells were transformed with either the two plasmids pKA1/*alkJ* and pET16b/*fsa1-A129S*, or one of the vectors for coexpression described above. Although the empty-host control *E. coli* BL21(DE3) and the transformants did not show different growth behavior in rich medium (lysogeny broth (LB) Miller; Figure S2a in the Supporting Information), (subtle) differences could be determined by monitoring bacterial growth in minimal medium (M9-N*; Figure S2b). Unburdened *E. coli* BL21 (DE3) showed short initial lag phases ($t_{(growth\ max)}$ after 7.6 h), followed by *E. coli* cells containing the POP plasmid (Table 2 and Figure S3). The two-plasmid system grew slower due to the higher plasmid burden, which was depicted by the maximal growth rate and shorter lag phases with all engineered configurations (Table 2). For further characterization, expression studies were performed under the optimized conditions for the two-plasmid system in M9-N* medium (25 °C, 150 rpm, 1 mM $ZnCl_2$, 0.5 mM isopropyl β-D-1-thiogalactopyranoside (IPTG)). Enzyme production was monitored over time (0–19 h) by SDS-PAGE analysis, and the results are shown in Figure 3 for exemplary whole-cell preparations of *E. coli* BL21(DE3) harboring the newly assembled plasmids. In all expression studies, AlkJ was readily produced and exclusively found in insoluble fractions because it was a membrane-associated protein (Figure 3).[26]

The production of Fsa1-A129S was strongly influenced by different genetic architectures and the inclusion of regulatory

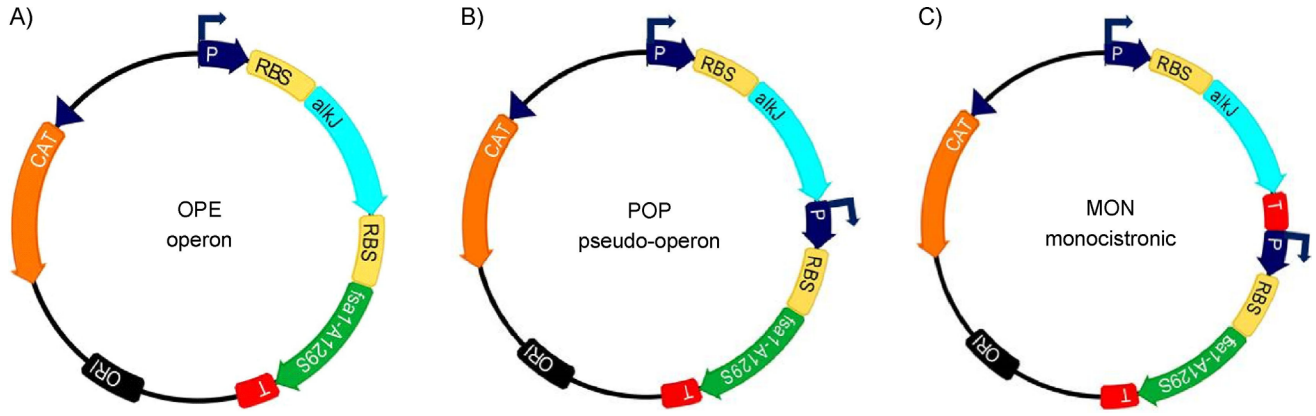

Figure 2. Illustration of genetic arrangements of AlkJ and Fsa1-A129S on single plasmids. A) Operon (OPE): one promoter (P) and a terminator (T). B) Pseudo-operon (POP): two Ps and one T. C) Monocistronic configuration (MON): two Ps and two Ts; ORI: origin of replication; RBS: ribosome binding site; CAT: chloramphenicol acetyltransferase. Figure adapted from Bayer et al.[20]

Table 2. Growth behavior of wild type and different transformants and Fsa1-A129S expression.

Vector	Growth rate [h^{-1}]	*t*(growth max) [h]	Fold change of soluble Fsa1-A129[a]
empty host BL21(DE3)	0.66	7.6	–
pKA1/*alkJ*	0.56	11.6	–
pKA1/*alkJ* pET16b/*fsa1-A129S*	0.55	11.5	1
OPE	0.70	8.8	0.50 ± 0.32
POP	0.76	7.7	1.02 ± 0.12
MON	0.66	8.8	0.94 ± 0.29

[a] Bradford assay was performed for Fsa1-A129S after purification by heat shock (HS). Normalization: cell pellet [g]; results represented as mean values of triplicates ± standard deviation (SD).

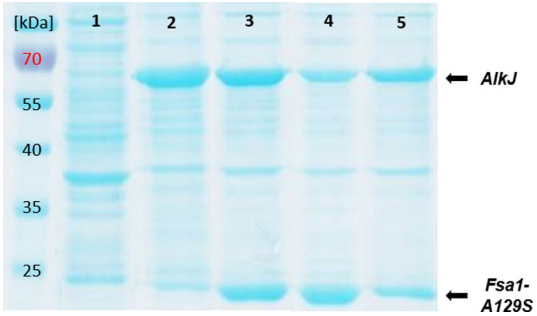

Figure 3. SDS-PAGE analysis of different genetic constructs. Whole-cell extracts from 1) untransformed *E. coli* BL21(DE3) and cells harboring 2) the OPE plasmid, 3) the POP plasmid, 4) the MON plasmid, and 5) the two-plasmid system. The production of AlkJ and Fsa1-A129S is indicated by arrows; sample loading normalized to $OD_{590} = 7.0$.

elements, as determined by protein quantification after isolation and heat shock (HS) purification of Fsa1-A129S preparations in comparison to the two plasmid system (pKA1/*alkJ* and pET16b/*fsa1-A129S*; Table 2).

Fsa1-A129S was poorly produced from the OPE plasmid simply because the distance between P_{T7} in front of the *alkJ* gene and the aldolase-coding region was too great. The production of soluble Fsa1-129S was improved when featuring an individual P_{T7} upstream of the RBS, as in the POP and the MON plasmids.[25] Based on beneficial growth behavior and the stable production of soluble Fsa1-A129S (Table 2), POP transformants of *E. coli* BL21(DE3) and the recently published reduced aromatic aldehyde reduction (RARE) strain were used for pathway validation and subsequent optimization of process parameters. The RARE strain consists of six rational gene knock-outs of aldo–keto reductase and ADHs, which results in an aldehyde-accumulating strain.[30]

Process parameter optimization—Substrate flux to product titers

After pathway construction and successful optimization at the genetic level, we focused on the productivity of our synthetic cascade. Based on the results presented above (e.g., growth rate and enzyme expression levels; Table 2), the pseudo-operon configuration was selected for further experiments (BL21(DE3) and RARE, 5 mM **1a**). As previously demonstrated, increasing concentrations of DHA (5 and 20 equiv) pushed the equilibrium of the aldol reaction toward the aldol adduct site and stably maintained target compounds, such as **2d**, over long reactions times (24 h) in resting cells (RCs) of *E. coli* BL21(DE3) harboring the POP plasmid (Figure 4B and C).[18a] In the absence of DHA, primary alcohol **1a** was almost completely overoxidized to the corresponding carboxylic acid, **1c** (Figure 4A). The same trend was observed with HA as the aldol donor (Figure S4). A large DHA/HA excess of 20 equivalents had a significant effect on the product stability because the reaction equilibrium was pushed toward the aldol adduct side. This was in marked contrast to the reaction with five equivalents of donor molecule, in which the freely available aldehyde species was converted into the carboxylate by-product **1c**, directing the carbon flux into a dead end.[18a] The same set of experiments was performed with *E. coli* RARE transformed with the POP construct (Figure 4D–F). In contrast to that of *E. coli* BL21(DE3), the persistence of aldehyde led to the rapid formation of the desired aldol adduct **1d**, even with five equivalents of DHA in 2 h reaction time. More striking is the fact that the retro-aldol reaction was slowed down significantly, presumably due to reduced overoxidation towards **1c**, which would pull the equilibrium towards the retro-aldol side (Figure 4E). In the presence of 20 equivalents of DHA, the reaction performance was comparable to that of *E. coli* BL21(DE3) transformants. Highest aldol yields (**1d**) were detected after 2 h reaction time.

The combination of whole-cell biocatalysts and a large excess (20 equiv) of the cheap aldol donor DHA gave perfect substrate conversion within 2 h, reducing carboxylate by-product formation and demonstrating an efficient pathway setup for the synthesis of the polyhydroxylated target molecule, **1d**. Next, the whole-cell biocatalyst and improved reaction settings were applied to our substrate portfolio (**1**–**4a**) to perform preparative biotransformations. The BL21(DE3) strain is more robust with respect to plasmid maintenance and has higher growth rates (Figure S2C). Protein levels were generally higher and biotransformations more reproducible than that with the RARE strain (Figure S1).

Isolation and purification by SPE

Acyclic aldol products are temperature sensitive (decomposition at room temperature within 48 h) and highly water soluble. Hence, their isolation and purification are particularly challenging and represent the yield-determining step.[9a,27,31]

We investigated different established isolation and purification methods and compared the results to our refined SPE protocol (Table 3, **1**–**4d**; for **1e** no literature data are available).[18a] To identify a suitable isolation method, purified Fsa1-A129S lyophilizates were used for stereoselective C–C bond formation between the corresponding aldehydes (**1**–**4b**) and DHA monomer (4 equiv) or HA (1.5 equiv) in 50 mM borate buffer (pH 7.0).[27] Reactions were monitored by GC/FID and HPLC analysis and stopped after full conversion to the target aldol adduct (**1**–**4d**, **e**).

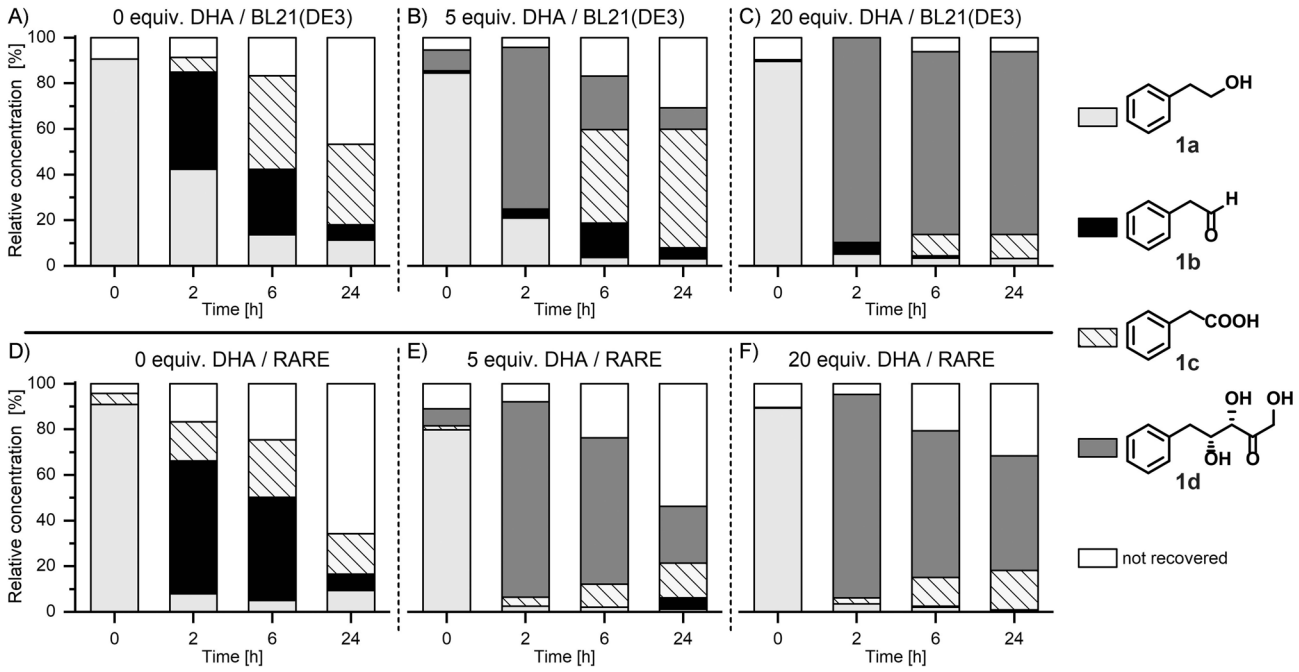

Figure 4. Conversion of 5 mM **1a** in RCs (OD_{590} = 10.0) coexpressing AlkJ and Fsa1-A129S from the POP plasmid in *E. coli* BL21(DE3) at DHA concentrations of A) 0, B) 5, and C) 20 equiv or in *E. coli* RARE at DHA concentrations of D) 0, E) 5, and F) 20 equiv. DHA was monomerized in RC medium. Reaction process was monitored by GC/FID and HPLC at t = 0* (immediately after mixing) and after 2, 6, and 24 h reaction time. All results are presented as mean values of biological triplicates with SDs of < 10 and < 5%, according to calibrated GC and HPLC, respectively.

Table 3. Comparison of different purification strategies with respect to isolated yield.

Target molecule	Donor	Product	Yield [%][a] A	B	C	D (Lit.)
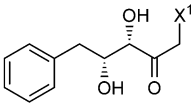	DHA	**1d**	n.a.	28	78	46[b]
	HA	**1e**	40	–	70	48[b]
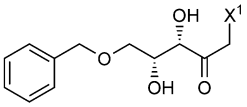	DHA	**2d**	n.a.	37	60	28[b]
	HA	**2e**	22	42	89	71[b]
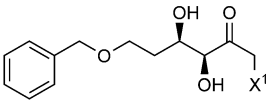	DHA	**3d**	n.a.	18	64	n.a.
	HA	**3e**	20	21	61	n.a.
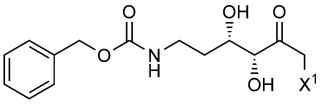	DHA	**4d**	n.a.	35	91	79[c]
	HA	**4e**	n.a.	32	83	n.a.

[a] 10% water content based on ^{1}H NMR spectroscopy experiments in [D_4]MeOH and [D_6]DMSO (see Tables S16 and S17); A: centrifugation, extraction of the supernatant with dichloromethane or ethyl acetate, and purification by preparative HPLC; B: reaction quenched with methanol ($2 \times V_R$), centrifugation, supernatant concentration, dissolution in methanol (product solubility was monitored by TLC), and purification by preparative HPLC; C: centrifugation and supernatant purification by SPE; n.a.: not applicable. [b] Published yields with purified Fsa1-A129S lyophilizates.[31] [c] In vitro HL-ADH from horse liver/nicotinamide adenine dinucleotide (NADH) oxidase/Fsa1-A129S.[27]

Simple extraction with organic solvents (dichloromethane or ethyl acetate; Table 3, A) was initially investigated and turned out only to be feasible for less hydrophilic HA aldol adducts **1**–**4e**, but failed for highly water-soluble products **1**–**4d**.

These results prompted us to apply a preparative reversed-phase (RP) HPLC (C_{18} material) protocol (Table 3, B). As observed previously, this method resulted in only moderate yields for the HA aldol adducts **1**–**4e**, but gave access to the

more hydrophilic DHA products **1**–**4 d**. The limitations of method B originate from the concentration/lyophilization steps and poor product solubility in the presence of buffer salts. To separate these highly water soluble and interfering components, we applied a simple SPE protocol (Table 3, C).

The absence of elaborate sample preparation steps represents the most prominent advantage of the SPE purification protocol, which prevents product decomposition. After the biotransformation was completed, cells were centrifuged and the supernatant was continuously transferred onto a short C_{18} column (Figure S4). First, all buffer salts and reaction by-products were eluted with a 95%/5% mixture of H_2O/methanol and monitored by using an evaporative light-scattering detector (ELSD) in combination with a UV detector ($\lambda = 205$ nm; Figure S5). After changing the mobile phase to 95% methanol, the pure products were eluted and concentrated under reduced pressure at room temperature (Table 3, C).

The entire SPE purification was performed in less than 1 h in good to very good yields; product purity was confirmed by NMR spectroscopy and LC/MS. The use of methanol as a solvent is also beneficial for the subsequent transformation towards D-fagomine, since it is one of the most prominent solvents applied in catalytic hydrogenations. The eluent of the SPE purification can be used directly without any further treatment.[9a]

Herein, we tackled a neglected but very important issue in the synthesis of polyhydroxylated compounds. Upon isolation of the target products we realized that all obtained adducts tended to form the monohydrate, which had a severe influence on the overall yield of product isolated. We applied orthogonal analytical methods—GC, HPLC, and NMR spectroscopy—to substantiate our hypothesis and validate our experimental results. A detailed experimental confirmation is given in the Supporting Information.

Based on the gained knowledge described above, we evaluated the efficiency of the SPE purification method and compared it with previously reported results (Table 3, D). In summary, our SPE protocol yielded significantly higher amounts (up to 91% or 4.55 mM yield after two steps) of the corresponding aldol adducts than that reported in the literature.

Conclusion

We successfully developed a sustainable and protection-group-free biocatalytic synthetic cascade in the model organism *E. coli* for the asymmetric synthesis of polyhydroxylated molecules. We applied the concept of in situ aldehyde production by the combination of the ADH AlkJ and the engineered aldolase Fsa1-A129S to avoid high intracellular concentrations of cytotoxic aldehyde species; thereby enabling transformations from cheap and more stable primary alcohol precursors and minimizing side reactions. Optimization at the genetic level by assembling both pathway genes, *alkJ* and *fsa1-A129S*, on a single plasmid, combined with improved biotransformation conditions, greatly enhanced the overall performance of the synthetic "mini" pathway. Finally, we developed an easy to apply and scalable SPE isolation and purification protocol, which led to product yields of up to 91% over two reaction steps in short reaction times. In contrast to our previously reported proof of concept study,[18a] we emphasized the cooperative effects of multiple optimization strategies for the design of microbial cell factories and yield maximization of artificial pathways in asymmetric synthesis.

Experimental Section

Materials and equipment: Unless noted otherwise, all reagents were purchased from commercial suppliers and used without further purification. Chromatography solvents were distilled prior to use. For all other solvents, quality grade is given in the reaction procedures. NMR spectra were recorded as solutions in $CDCl_3$, D_2O, [D_6]DMSO, or [D_4]MeOH on Bruker AC 200 (200 MHz), Bruker Advance UltraShield 400 (400 MHz), or Bruker Avance IIIHD (600 MHz) spectrometers and chemical shifts are reported in ppm by using tetramethylsilane as an internal standard (IS). Whenever possible, calibration through residual solvent signals was performed. Signal assignment is based on correlation experiments or software prediction. GC analysis was performed on a Thermo Finnigan Focus GC/DSQ II by using an RXi-5Sil MS (15 m × 0.25 mm i.d., 0.1 μm film) column with a Thermo Focus GC/FID detector. The injected sample volume was 1 μL. LC/MS analysis was performed by using a HPLC instrument (Nexera, Shimadzu). The injected volume of the samples was 10 μL. Supernatants were analyzed with a photodiode array detector (PDA) for quantification of analytes at $\lambda = 190$ nm; a refractive index (RI) detector and ESI ion source with a quadrupole mass analyzer (LC/MS 2020 Shimadzu) were used for additional confirmation of the substances. Separation was performed with an ROA-Organic Acid H+ (8%) column (150 × 7.8 mm, Phenomenex) with an isocratic flow of 0.5 mL min^{-1} of 0.1% (*v*/*v*) formic acid in water (HPLC grade). HRMS analysis was performed from solutions in methanol (concentration: 10 ppm) by using an HTC PAL system autosampler (CTC Analytics AG, Zwingen, Switzerland); an Agilent 1100/1200 HPLC with binary pumps, degasser, and column thermostat (Agilent Technologies, Waldbronn, Germany); and an Agilent 6230 AJS ESI-TOF mass spectrometer (Agilent Technologies, Palo Alto, United States). Column chromatography was performed on a BUCHI Sepacore Flash System (2 × BUCHI Pump Module C-605, BUCHI Pump Manager C-615, BUCHI UV Photometer C-635, BUCHI Fraction Collector C-660) by using mixtures of dichloromethane and ethyl acetate. SPE purification was performed on a Grace REVELERIS X flash chromatography system with integrated ELS/UV/UV/Vis detection by using a BUCHI Sepacore Flash Cartridge (C18; 25 g) and HPLC-grade water or methanol. Preparative column chromatography was performed on a Waters autopurification system (2545 (Binary gradient module); SFO (System fluidics organizer); 2767 (Sample manager)) by using an xSelect CSHTM C_{18} 5 μm (4.6 mm × 150 mm) column on an Acquity QDa detector.

Enzyme expression from the POP plasmid and preparation of RCs: For enzyme expression, a single colony of the desired *E. coli* transformant was incubated in LB-0.8G medium (10 mL; 10 g L^{-1} bactopeptone, 5 g L^{-1} yeast extract, 10 g L^{-1} NaCl, 1 mM $MgSO_4$, 0.8% (*w*/*v*) glucose, 25 mM $(NH_4)_2SO_4$, 50 mM KH_2PO_4, 50 mM Na_2HPO_4) supplemented with chloramphenicol (34 μg mL^{-1}) at 37 °C with shaking (275 rpm; InforsHT Multitron 2 Standard) overnight. Autoinduction medium (AIM; 10 g L^{-1} bactopeptone, 5 g L^{-1} yeast extract, 10 g L^{-1} NaCl, 1 mM $MgSO_4$, 5.0% (*w*/*v*) glycerol, 0.5% (*w*/*v*) glucose, 2.0% (*w*/*v*) α-lactose, 25 mM $(NH_4)_2SO_4$, 50 mM KH_2PO_4, 50 mM Na_2HPO_4) supplemented with chloramphenicol was inoculated with 0.2% (*v*/*v*) of the preculture and incubated at 37 °C

with shaking (150 rpm) for 4 h. The temperature was lowered to 20 °C and the main culture shaken for 20 h. The preparation of AIM was in accordance with the method reported by Studier.[32] For RC preparation, cells were harvested by centrifugation (6000 *g* at 4 °C, 15 min; Sigma laboratory centrifuge 6k15). The pellet was washed with RC medium (1% (*w*/*v*) glucose, 8.6 mM NaCl, 42 mM Na_2HPO_4, 22 mM KH_2PO_4, 3 mM $MgSO_4$, 0.1 mM $CaCl_2$, 0.06 mM $FeCl_3$, 0.002 mM thiamine·HCl) and centrifuged. The washed cell pellet was resuspended in a sufficient volume of RC medium until OD_{590} = 20.0 was reached. RCs were stored at 4 °C for up to 1 day.[18a]

General screening procedure with RCs coexpressing AlkJ and Fsa1-A129S: RCs of the *E. coli* transformant (POP) were prepared as described above and analytical biotransformations were performed in 8 mL vials fitted with screw caps. RCs were used at OD_{590} = 10.0 for all screenings. The substrate was added last from 100 mM stock solutions in pure organic solvent (HPLC-grade MeCN), the vial was closed, and mixing was achieved by inversion six times. Reaction mixtures were incubated at 25 °C with shaking (250 rpm). Screening samples were taken at t = 0* (immediately after mixing) and after 0, 2, 6, and 24 h of incubation. For GC analysis, the reaction mixture (100 μL) was added to 1.5 mL Eppendorf tubes containing HCl (10 μL, 2 N) and EtOAc (200 μL; HPLC grade) supplemented with 1 mM methyl benzoate as IS. The mixture was vortexed at maximum speed for 30–35 s and spun down for 1 min (VWR Silverstar bench-top centrifuge). The organic layer was transferred into a new 1.5 mL tube and the aqueous layer was extracted again with EtOAc (190 μL) containing IS (1 mM). The combined organic layers were dried over Na_2SO_4 and analyzed by GC/FID. For HPLC analysis, the reaction mixture (200 μL) was transferred into 1.5 mL Eppendorf tubes and solid biotransformation material was separated by centrifugation (6000 *g*, 4 °C, 10 min). The obtained supernatant was filtered through a 0.2 μm polytetrafluoroethylene (PTFE) membrane syringe filter (4552T, Pall Life Sciences) in a 1.5 mL glass vial equipped with a microinlet and analyzed by HPLC.

Preparative biotransformations by using POP transformants in the presence of DHA or HA: RCs of *E. coli* BL21(DE3) coexpressing AlkJ and Fsa1-A129S were prepared as described previously. In the case of DHA, dimer (1.8 g) was monomerized in RC medium (20 mL) for 2 h at 37 °C in an orbital shaker (200 rpm). In a 1 L baffled Erlenmeyer flask, the aldol acceptor molecule (1 equiv, 1.0 mmol) was dissolved in MeCN (10 mL) and the DHA or HA monomer solution (20 equiv, 20 mmol) was added to freshly prepared RCs (OD_{590} = 10.0) and shaken at 25 °C, 250 rpm (V_{total} = 200 mL). The reaction progress was monitored by GC/FID or RP-TLC (MeOH/H_2O 3:1), until full consumption of the starting material was observed. The crude reaction mixture was centrifuged and directly transferred for purification on a BUCHI Sepacore flash cartridge (C_{18}, 25 g). RC media ingredients (e.g., salts) and excess DHA were eluted with MeOH/H_2O (5:95, *v*/*v*) followed by product elution with 100% methanol. The product fractions were concentrated at 25–30 °C under high vacuum to obtain the pure product.

(3*S*,4*R*)-1,3,4-Trihydroxy-5-phenylpentan-2-one (1 d): Colorless oil; 163 mg (78%); $[\alpha]_D$ = 21.8 (c = 1.07 in $CHCl_3$; lit.[33] $[\alpha]_D$ = 26.7 (c = 1.07 in $CHCl_3$)); ^{1}H NMR (400 MHz, [D$_4$]MeOH): δ = 2.84 (dd, J = 13.4, 7.4 Hz, 1H), 2.94 (dd, J = 13.4, 7.1 Hz, 1H), 4.04 (d, J = 2.2 Hz, 1H), 4.14 (td, J = 7.2, 2.1 Hz, 1H), 4.41–4.54 (m, 2H), 7.17–7.31 ppm (m, 5H); ^{13}C NMR (101 MHz, [D$_4$]MeOH): δ = 40.7, 67.9, 75.0, 78.3, 127.4, 129.4, 130.5, 139.8, 214.02 (s, C2);[27] LC/MS (ESI$^+$): *m*/*z* calcd for $C_{11}H_{14}O_4$: 233.07 [*M*+Na]$^+$, found 233.05.

(3*S*,4*R*)-3,4-Dihydroxy-5-phenylpentan-2-one (1 e): Colorless oil; 135 mg (70%); $[\alpha]_D$ = 31.7 (c = 1.0 in methanol; lit.[27] $[\alpha]_D$ = 29.8 (c = 1.0 in methanol)); ^{1}H NMR (400 MHz, [D$_4$]MeOH): δ = 2.18 (s, 3H) 2.86 (dd, J = 13.3, 7.4 Hz, 1H), 2.96 (dd, J = 13.3, 7.0 Hz, 1H), 3.94 (d, J = 2.0 Hz, 1H) 4.14–4.19 (m, 1H), 7.17–7.30 ppm (m, 5H); ^{13}C NMR (101 MHz, [D$_4$]MeOH): δ = 26.5, 41.0, 74.7, 79.7, 127.3, 129.4, 130.5, 139.8, 212.4 ppm;[27] LC/MS (ESI$^+$): *m*/*z*: calcd for $C_{11}H_{14}O_3$: 217.08 [*M*+Na]$^+$, found 217.07.

5-*O*-Benzyl-D-xylulose (2 d): Colorless oil; 142 mg (60%); $[\alpha]_D$ = 5.3 (c = 1.0 in $CHCl_3$; lit.[27] $[\alpha]_D$ = 2.8 (c = 1.0 in $CHCl_3$)); ^{1}H NMR (400 MHz, [D$_4$]MeOH) δ = 3.53 (dd, J = 9.6, 6.1 Hz, 1H), 3.63 (dd, J = 9.6, 6.6 Hz, 1H), 4.12 (td, J = 6.5, 1.8 Hz, 1H), 4.31 (d, J = 2.0 Hz, 1H), 4.43–4.57 (m, 2H), 4.55 (s, 2H), 7.24–7.37 ppm (m, 5H); ^{13}C NMR (101 MHz, [D$_4$]MeOH): δ = 67.9, 71.6, 72.1, 74.3, 77.2, 128.7, 128.8, 129.3, 129.6, 130.6, 139.6, 213.5 ppm;[27] LC/MS (ESI$^+$): *m*/*z* calcd for $C_{12}H_{16}O_5$: 263.08 [*M*+Na]$^+$, found 263.05.

5-*O*-Benzyl-1-deoxy-D-xylulose (2 e): Colorless oil; 199 mg (89%); $[\alpha]_D$ = 51.9 (c = 1.0 in CH_2Cl_2; lit.[27] $[\alpha]_D$ = 58.2 (c = 1.0 in CH_2Cl_2)); ^{1}H NMR (600 MHz, [D$_4$]MeOH) δ = 2.24 (s, 3H), 3.56 (dd, J = 9.5, 6.2 Hz, 1H), 3.66 (dd, J = 9.5, 6.5 Hz, 1H), 4.17 (td, J = 6.3, 2.3 Hz, 1H), 4.22 (d, J = 2.4 Hz, 1H), 4.55–4.59 (m, 2H), 7.28–7.39 ppm (m, 5H); ^{13}C NMR (151 MHz, [D$_4$]MeOH): δ = 26.6, 71.8, 71.9, 74.3, 78.7, 128.7, 128.9, 129.3, 129.4, 139.6, 212.0 ppm;[27] LC/MS (ESI$^+$): *m*/*z* calcd for $C_{12}H_{16}O_4$: 247.09 [*M*+Na]$^+$, found 247.06.

(3*S*,4*R*)-6-(Benzyloxy)-1,3,4-trihydroxyhexan-2-one (3 d): Colorless oil; 162 mg (64%); $[\alpha]_D$ = 5.8 (c = 1.0 in methanol); ^{1}H NMR (600 MHz, [D$_4$]MeOH): δ = 1.90 (m, 2H), 3.58–3.66 (m, 2H), 4.13–4.15 (m, 2H), 4.43–4.55 (m, 4H), 7.25–7.35 ppm (m, 5H); ^{13}C NMR (151 MHz, [D$_4$]MeOH): δ = 34.3, 67.8, 68.1, 70.8, 74.0, 79.4, 128.6, 128.8, 129.4, 139.7, 213.5 ppm; HRMS (ESI$^+$): *m*/*z* calcd for $C_{13}H_{18}O_5$ [*M*+Na]$^+$: 277.1046, found: 277.1044.

(3*S*,4*R*)-6-(Benzyloxy)-3,4-dihydroxyhexan-2-one (3 e): Colorless oil; 144 mg (61%); $[\alpha]_D$ = 45.1 (c = 1.0 in methanol); ^{1}H NMR (600 MHz, [D$_4$]MeOH): δ = 1.87–1.90 (m, 2H), 2.21 (s, 3H), 3.57–3.68 (m, 2H), 4.02 (d, J = 2.3 Hz, 1H), 4.17 (td, J = 6.2, 2.3 Hz, 1H), 4.53–4.56 (m, 2H), 7.26–7.36 ppm (m, 5H); ^{13}C NMR (151 MHz, [D$_4$]MeOH): δ = 26.6, 34.6, 68.1, 70.4, 74.0, 81.0, 128.7, 128.9, 129.4, 139.7, 212.0 ppm; HRMS (ESI$^+$): *m*/*z* calcd for $C_{13}H_{18}O_4$: 261.1097 [*M*+Na]$^+$, found: 261.1108.

L-*threo*-2-Hexulose-5,6-drideoxy-6-[(phenylmethoxy)carbonyl]amino (4 d): Colorless oil; 270 mg (91%); $[\alpha]_D$ = 5.8 (c = 1.0 in methanol; lit.[34] $[\alpha]_D$ = 9.0 (c = 1.0 in methanol)); ^{1}H NMR (400 MHz, [D$_4$]MeOH): δ = 1.73–1.79 (m, 2H), 3.19–3.27 (m, 2H), 3.98 (td, J = 8.1, 2.4 Hz, 1H), 4.13 (d, J = 2.3 Hz, 1H), 4.43–4.52 (m, J = 19.2 Hz, 2H), 5.07 (s, 2H), 7.26–7.37 ppm (m, 5H); ^{13}C NMR (101 MHz, [D$_4$]MeOH): δ = 34.4, 38.7, 67.4, 67.8, 71.1, 79.4, 128.8, 129.0, 129.5, 138.4, 159.0, 213.4 ppm; LC/MS (ESI$^+$): *m*/*z* calcd for $C_{14}H_{19}NO_6$: 320.10 [*M*+Na]$^+$, found 320.11.

L-*threo*-2-Hexulose-1,5,6-trideoxy-6-[(phenylmethoxy)carbonyl]amino (4 e): Colorless oil; 233 mg (83%); $[\alpha]_D$ = 50.5 (c = 1.0 in CH_2Cl_2); ^{1}H NMR (400 MHz, [D$_4$]MeOH): δ = 1.75–1.80 (m, 2H), 2.20 (s, 3H), 3.20–3.29 (m, 2H), 4.01 (td, J = 6.8, 2.3 Hz, 1H), 4.05 (d, J = 2.3 Hz, 1H), 5.07 (s, 2H), 7.27–7.37 ppm (m, 5H); ^{13}C NMR (101 MHz, [D$_4$]MeOH): δ = 26.5, 34.7, 38.7, 67.4, 70.7, 80.9, 128.8, 128.9, 129.4, 138.4, 159.0, 211.9 ppm; LC/MS (ESI$^+$): *m*/*z* calcd for $C_{14}H_{19}NO_6$: 304.11 [*M*+Na]$^+$, found 304.12.

Acknowledgements

We would like to thank W.-D. Fessner (University of Technology Darmstadt) for supplying the gene encoding Fsa1-A129S and B. Buehler (UFZ Leipzig) for the gene encoding AlkJ. We thank the FWF (grant no. P24483_B20) and the COST action Systems Biocatalysis WG2.

Conflict of Interest

The authors declare no conflict of interest.

Keywords: alcohols · biocatalysis · domino reactions · enzymes · solid-phase extraction

[1] a) D. B. Werz, P. H. Seeberger, *Chem. Eur. J.* **2005**, *11*, 3194 – 3206; b) A. Fernández-Tejada, F. J. Canada, J. Jimenez-Barbero, *Chem. Eur. J.* **2015**, *21*, 10616 – 10628; c) B. Lepenies, J. A. Yin, P. H. Seeberger, *Curr. Opin. Chem. Biol.* **2010**, *14*, 404 – 411.

[2] a) A. Höleman, P. H. Seeberger, *Curr. Opin. Biotechnol.* **2004**, *15*, 615 – 622; b) V. L. Campo, V. Aragao-Leoneti, M. B. M. Teixeira, I. Carvalho, *New Dev. Med. Chem.* **2010**, *1*, 133 – 151; c) C. R. Bertozzi, L. L. Kiessling, *Science* **2001**, *291*, 2357 – 2364.

[3] M. C. Galan, D. Benito-Alifonso, G. M. Watt, *Org. Biomol. Chem.* **2011**, *9*, 3598 – 3610.

[4] T. Hudlicky, D. A. Entwistle, K. K. Pitzer, A. J. Thorpe, *Chem. Rev.* **1996**, *96*, 1195 – 1220.

[5] a) J. Mlynarski, B. Gut, *Chem. Soc. Rev.* **2012**, *41*, 587 – 596; b) C. Palomo, M. Oiarbide, J. M. Garcia, *Chem. Soc. Rev.* **2004**, *33*, 65 – 75; c) M. Markert, R. Mahrwald, *Chem. Eur. J.* **2008**, *14*, 40 – 48.

[6] a) A. B. Northrup, I. K. Mangion, F. Hettche, D. W. C. MacMillan, *Angew. Chem. Int. Ed.* **2004**, *43*, 2152 – 2154; *Angew. Chem.* **2004**, *116*, 2204 – 2206; b) A. B. Northrup, D. W. C. MacMillan, *Science* **2004**, *305*, 1752 – 1755.

[7] A. Szekrenyi, X. Garrabou, T. Parella, J. Joglar, J. Bujons, P. Clapés, *Nat. Chem.* **2015**, *7*, 724 – 729.

[8] P. Clapés, W. D. Fessner, G. A. Sprenger, A. K. Samland, *Curr. Opin. Chem. Biol.* **2010**, *14*, 154 – 167.

[9] a) M. Wei, Z. Li, T. Li, B. Wu, Y. Liu, J. Qu, X. Li, L. Li, L. Cai, P. G. Wang, *ACS Catal.* **2015**, *5*, 4060 – 4065; b) O. Eyrisch, W. D. Fessner, *Angew. Chem. Int. Ed. Engl.* **1995**, *34*, 1639 – 1641; *Angew. Chem.* **1995**, *107*, 1738 – 1740; c) M. D. Bednarski, E. S. Simon, N. Bischofberger, W. D. Fessner, M. J. Kim, W. Lees, T. Saito, H. Waldmann, G. M. Whitesides, *J. Am. Chem. Soc.* **1989**, *111*, 627 – 635; d) A. N. Phung, M. T. Zannetti, G. Whited, W. D. Fessner, *Angew. Chem. Int. Ed.* **2003**, *42*, 4821 – 4824; *Angew. Chem.* **2003**, *115*, 4970 – 4972; e) L. Gómez, X. Garrabou, J. Joglar, J. Bujons, T. Parella, C. Vilaplana, P. J. Cardona, P. Clapés, *Org. Biomol. Chem.* **2012**, *10*, 6309 – 6321; f) X. Garrabou, J. A. Castillo, C. Guerard-Helaine, T. Parella, J. Joglar, M. Lemaire, P. Clapés, *Angew. Chem. Int. Ed.* **2009**, *48*, 5521 – 5525; *Angew. Chem.* **2009**, *121*, 5629 – 5633; g) I. Oroz-Guinea, K. Hernandez, F. C. Bres, C. Guerard-Helaine, M. Lemaire, P. Clapés, E. Garcia-Junceda, *Adv. Synth. Catal.* **2015**, *357*, 1951 – 1960; h) F. Camps Bres, C. Guerard-Helaine, V. Helaine, C. Fernandes, I. Sanchez-Moreno, M. Traikia, E. Garcia-Junceda, M. Lemaire, *J. Mol. Catal. B* **2015**, *114*, 50 – 57.

[10] J. A. Castillo, C. Guerard-Helaine, M. Gutierrez, X. Garrabou, M. Sancelme, M. Schurmann, T. Inoue, V. Helaine, F. Charmantray, T. Gefflaut, L. Hecquet, J. Joglar, P. Clapés, G. A. Sprenger, M. Lemaire, *Adv. Synth. Catal.* **2010**, *352*, 1039 – 1046.

[11] A. Szekrenyi, A. Soler, X. Garrabou, C. Guerard-Helaine, T. Parella, J. Joglar, M. Lemaire, J. Bujons, P. Clapés, *Chem. Eur. J.* **2014**, *20*, 12572 – 12583.

[12] D. Güclü, A. Szekrenyi, X. Garrabou, M. Kickstein, S. Junker, P. Clapés, W. D. Fessneer, *ACS Catal.* **2016**, *6*, 1848 – 1852.

[13] A. Soler, M. L. Gutierrez, J. Bujons, T. Parella, C. Minguillon, J. Joglar, P. Clapés, *Adv. Synth. Catal.* **2015**, *357*, 1787 – 1807.

[14] M. Sudar, Z. Findrik, D. Vasic-Racki, A. Soler, P. Clapés, *RSC Adv.* **2015**, *5*, 69819 – 69828.

[15] a) S. Herter, S. M. McKenna, A. R. Frazer, S. Leimkuhler, A. J. Carnell, N. J. Turner, *ChemCatChem* **2015**, *7*, 2313 – 2317; b) M. Mifsud, A. Szekrenyi, J. Joglar, P. Clapés, *J. Mol. Catal. B* **2012**, *84*, 102 – 107.

[16] J. H. Schrittwieser, S. Velikogne, M. Hall, W. Kroutil, *Chem. Rev.* **2017**, https://doi.org/10.1021/acs.chemrev.7b00033.

[17] a) W. D. Fessner, *New Biotechnol.* **2014**, *31*, S74 – S74; b) W. D. Fessner, *New Biotechnol.* **2015**, *32*, 658 – 664.

[18] a) T. Bayer, S. Milker, T. Wiesinger, M. Winkler, M. D. Mihovilovic, F. Rudroff, *ChemCatChem* **2017**, *9*, 2919 – 2923; b) J. Muschiol, C. Peters, N. Oberleitner, M. D. Mihovilovic, U. T. Bornscheuer, F. Rudroff, *Chem. Commun.* **2015**, *51*, 5798 – 5811; c) V. Köhler, N. J. Turner, *Chem. Commun.* **2015**, *51*, 450 – 464.

[19] a) R. Agudo, M. T. Reetz, *Chem. Commun.* **2013**, *49*, 10914 – 10916; b) M. Schrewe, M. K. Julsing, B. Buhler, A. Schmid, *Chem. Soc. Rev.* **2013**, *42*, 6346 – 6377.

[20] T. Bayer, S. Milker, T. Wiesinger, F. Rudroff, M. D. Mihovilovic, *Adv. Synth. Catal.* **2015**, *357*, 1587 – 1618.

[21] A. Weckbecker, W. Hummel, *Biocatal. Biotransform.* **2006**, *24*, 380 – 389.

[22] "Purification and characterization of a secondary alcohol dehydrogenase ADH-A with high solvent and temperature stability from *Rhodococcus ruber*", W. Stampfer, B. Kosjek, W. Kroutil, K. Faber (CIBA Specialty Chemicals Holding Inc.), WO2003078615A1, **2003**.

[23] J. H. Sattler, M. Fuchs, K. Tauber, F. G. Mutti, K. Faber, J. Pfeffer, T. Haas, W. Kroutil, *Angew. Chem. Int. Ed.* **2012**, *51*, 9156 – 9159; *Angew. Chem.* **2012**, *124*, 9290 – 9293.

[24] C. Wuensch, H. Lechner, S. M. Glueck, K. Zangger, M. Hall, K. Faber, *ChemCatChem* **2013**, *5*, 1744 – 1748.

[25] M. Schrewe, M. K. Julsing, K. Lange, E. Czarnotta, A. Schmid, B. Bühler, *Biotechnol. Bioeng.* **2014**, *111*, 1820 – 1830.

[26] S. Wu, Y. Zhou, T. Wang, H.-P. Too, D. I. C. Wang, Z. Li, *Nat. Commun.* **2016**, *7*, 11917.

[27] A. L. Concia, C. Lozano, J. A. Castillo, T. Parella, J. Joglar, P. Clapés, *Chem. Eur. J.* **2009**, *15*, 3808 – 3816.

[28] C. Li, A. Wen, B. Shen, J. Lu, Y. Huang, Y. Chang, *BMC Biotechnol.* **2011**, *11*, 1 – 10.

[29] Y. Zhang, U. Werling, W. Edelmann, *Nucleic Acids Res.* **2012**, *40*, e55.

[30] A. M. Kunjapur, Y. Tarasova, K. L. J. Prather, *J. Am. Chem. Soc.* **2014**, *136*, 11644 – 11654.

[31] M. Sugiyama, Z. Hong, P. H. Liang, S. M. Dean, L. J. Whalen, W. A. Greenberg, C. H. Wong, *J. Am. Chem. Soc.* **2007**, *129*, 14811 – 14817.

[32] F. W. Studier, *Protein Expr. Purif.* **2005**, *41*, 207 – 234.

[33] A. J. Humphrey, N. J. Turner, R. McCague, S. J. C. Taylor, *J. Chem. Soc. Chem. Commun.* **1995**, 2475 – 2476.

[34] J. A. Castillo, J. Calveras, J. Casas, M. Mitjans, M. P. Vinardell, T. Parella, T. Inoue, G. A. Sprenger, J. Joglar, P. Clapés, *Org. Lett.* **2006**, *8*, 6067 – 6070.

Manuscript received: August 31, 2017

Accepted manuscript online: October 5, 2017

Version of record online: ■■ ■■, 0000

Cascades in cells: A synthetic cascade for the transformation of primary alcohols into polyhydroxylated compounds through in situ preparation of cytotoxic aldehyde intermediates and subsequent aldolase-mediated C–C bond formation is investigated. The optimized whole-cell catalyst, combined with a refined solid-phase extraction downstream purification protocol gives optically pure aldol products.

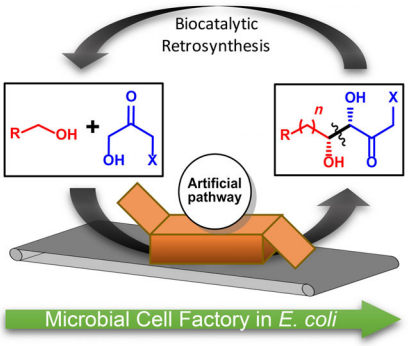

*T. Wiesinger, T. Bayer, S. Milker, M. D. Mihovilovic, F. Rudroff**

■■ – ■■

Cell Factory Design and Optimization for the Stereoselective Synthesis of Polyhydroxylated Compounds